HHS Public Access

Author manuscript

Mol Nutr Food Res. Author manuscript; available in PMC 2020 July 01.

Published in final edited form as:

Mol Nutr Food Res. 2020 April ; 64(8): e1900907. doi:10.1002/mnfr.201900907.

Influence of Diet-Induced Obesity on the Bioavailability and Metabolism of Raspberry Ketone (4-(4-Hydroxyphenyl)-2-Butanone) in Mice

Danyue Zhao[+],

New Use Agriculture and Natural Plant Products Program, Department of Plant Biology, School of Environmental and Biological Sciences, Rutgers University, New Brunswick, NJ 08901, USA

New Jersey Institute for Food, Nutrition and Health, Rutgers, The State University of New Jersey, New Brunswick NJ 08901, USA

Bo Yuan,

New Use Agriculture and Natural Plant Products Program, Department of Plant Biology, School of Environmental and Biological Sciences, Rutgers University, New Brunswick, NJ 08901, USA

Department of Food Science Rutgers University, 65 Dudley Road New Brunswick, NJ 08901, USA

Dushyant Kshatriya,

Department of Animal Sciences, School of Environmental and Biological Sciences, Rutgers, The State University of New Jersey, New Brunswick NJ 08901, USA

Nutritional Sciences Graduate Program, School of Environmental and Biological Sciences, Rutgers, The State University of New Jersey, New Brunswick NJ 08901, USA

Andrew Polyak,

New Use Agriculture and Natural Plant Products Program, Department of Plant Biology, School of Environmental and Biological Sciences, Rutgers University, New Brunswick, NJ 08901, USA

James E. Simon,

New Use Agriculture and Natural Plant Products Program, Department of Plant Biology, School of Environmental and Biological Sciences, Rutgers University, New Brunswick, NJ 08901, USA

New Jersey Institute for Food, Nutrition and Health, Rutgers, The State University of New Jersey, New Brunswick NJ 08901, USA

Nicholas T. Bello,

qlwu@sebs.rutgers.edu, ntbello@rutgers.edu.

[+]Present address: Department of Applied Biology and Chemical Technology, The Hong Kong Polytechnic University, Hong Kong

Author Contributions

D.Z., Q.W., and N.T.B. designed the study; D.K., D.Z., B.Y., and A.P. conducted the animal experiments, and D.Z., B.Y., and A.P. analyzed the biosamples, D.Z., B.Y., and Q.W. interpreted the data; D.Z. drafted the manuscript; J.E.S. proofread the manuscript. All authors contributed to the framing of the study, and contributed to editing and reviewing of this manuscript.

Conflict of Interest

The authors declare no conflict of interest.

Supporting Information

Supporting Information is available from the Wiley Online Library or from the author.

Department of Animal Sciences, School of Environmental and Biological Sciences, Rutgers, The State University of New Jersey, New Brunswick NJ 08901, USA

New Jersey Institute for Food, Nutrition and Health, Rutgers, The State University of New Jersey, New Brunswick NJ 08901, USA

Nutritional Sciences Graduate Program, School of Environmental and Biological Sciences, Rutgers, The State University of New Jersey, New Brunswick NJ 08901, USA

Qingli Wu

New Use Agriculture and Natural Plant Products Program, Department of Plant Biology, School of Environmental and Biological Sciences, Rutgers University, New Brunswick, NJ 08901, USA

New Jersey Institute for Food, Nutrition and Health, Rutgers, The State University of New Jersey, New Brunswick NJ 08901, USA

Department of Food Science Rutgers University, 65 Dudley Road New Brunswick, NJ 08901, USA

Abstract

Objectives—Raspberry ketone (RK) is the primary aroma compound in red raspberries and a dietary supplement for weight loss. This work aims to 1) compare RK bioavailability in male versus female, normal-weight versus obese mice; 2) characterize RK metabolic pathways.

Methods—Study 1: C57BL/6J male and female mice fed a low-fat diet (LFD; 10% fat) receive a single oral gavage dose of RK (200 mg kg^{-1}). Blood, brain, and white adipose tissue (WAT) are collected over 12 h. Study 2: Male mice are fed a LFD or high-fat diet (45% fat) for 8 weeks before RK dosing. Samples collected are analyzed by UPLC-MS/MS for RK and its metabolites.

Results—RK is rapidly absorbed ($T_{max} \approx 15$ min), and bioconverted into diverse metabolites in mice. Total bioavailability (AUC_{0-12h}) is slightly lower in females than males (566 vs 675 nmol mL^{-1} min^{-1}). Total bioavailability in obese mice is almost doubled that of control mice (1197 vs 679 nmol mL^{-1} min^{-1}), while peaking times and elimination half-lives are delayed. Higher levels of RK and major metabolites are found in WAT of the obese than normal-weight animals.

Conclusions—RK is highly bioavailable, rapidly metabolized, and exhibits significantly different pharmacokinetic behaviors between obese and control mice. Lipid-rich tissues, especially WAT, can be a direct target of RK.

Keywords

bioavailability; metabolism; obesity; raspberry ketones

1. Introduction

Raspberry ketone (RK), 4-(*p*-hydroxyphenyl)-2-butanone, is a naturally occurring aromatic phenolic compound derived from red raspberries (*Rubus idaeus*), accounting for the characteristic “raspberry flavor.” In small quantities, it is classified as a generally recognized as safe synthetic flavoring agent by the US Food and Drug Administration;[1–6] at higher doses, RK has been found to exhibit in vitro anti-lipogenic and in vivo weight-reducing

activities.[2,7,8] Previously, we demonstrated that male C57BL/6J mice orally administered with RK attenuated high-fat diet (HFD)-induced adipose gain and metabolic alteration associated with obesity.[9] Multi-ingredient dietary supplements containing RK have also been shown to reduce body weight and improve metabolic outcomes in overweight men and women on an 8-weelc exercise program.[10] Although RK is marketed in the United States as a weight loss supplement, the biological actions of RK as a potential obesity-preventative agent have not been fully characterized.

To further elucidate RK's bioefficacy and mechanisms of action, it is critical to investigate RK's absorption, distribution, metabolism, and excretion (ADME). To date, only one pioneering study by Sporstøl and Scheline examined the metabolism of RK by analyzing the urinary profile of oral RK and its proposed metabolites in male rats, guinea pigs, and rabbits. They found that following an acute oral dose, RK was rapidly excreted within 24 h and primarily reduced into raspberry alcohol in all species.[11] Despite these findings, the metabolism of RK has not been well characterized with respect to sex, diet, and metabolic status. The present study first aims to determine the PK parameters of RK and its major metabolites, and their distribution in plasma, select tissues, and urine in male and female mice. From the perspective of obesity prevention by RK, we also sought to investigate how the bioavailability and metabolism of RK are influenced by metabolic health status using a mouse model of HFD-induced obesity. Previous studies have suggested that metabolic conditions such as being obese or diabetic significantly affect bioavailability and bioactivity of phenolic-rich preparations.[12,13] For example, obese individuals normally show altered gastrointestinal mobility, xenobiotic metabolism, and microbial compositions, which can significantly impact phenolic bioavailability[14,15] In view of the effects that RK exerts on white adipose, we hypothesize that RK and its major metabolites will accumulate at higher levels in the white adipose tissue (WAT) of obese than normal-weight mice. In addition, as the recommended doses for commercial RK dietary supplement are at 400–1400 mg day^{-1} for adults, which are excessively higher than the dietary doses,[16] understanding the bioavailability and metabolism of RK will also be instrumental to the regulation and application of RK-enriched products to avoid adverse side effects.

2. Experimental Section

2.1. Standards and Reagents

Raspberry ketone (4-(4-hydroxyphenyl)-2-butanone; 99%; Sigma-Aldrich, St. Louis, MO, USA) was deposited in a dark, climate-controlled repository. Most phenolic standards (HPLC grade; refer to Table S1, Supporting Information for detailed standard information), *β*-glucuronidase from *Patella vulgata* (in contamination with sulfatase) and ascorbic acid were purchased from Sigma-Aldrich, unless otherwise specified. Dihydroferulic acid and 3,4-dihydroxybenzylideneacetone were from Alfa Aesar (Ward Hill, MA, USA). LC-MS grade acids and solvents including glacial acetic acid (AA), formic acid, water, acetonitrile (ACN), methanol (MeOH), and ethyl acetate were from Fisher Scientific (Pittsburgh, PA, USA).

2.2. Animals

Seven-weelc-old C57BL/6J mice (Jackson's Laboratories, Bar Harbor, ME) were pair housed and maintained on a 12-h light, 12-h dark cycle at in the animal facility of the Department of Animal Sciences, Rutgers University. Following acclimation, animals were given ad libitum access to a polyphenol-free low-fat diet (LFD; 3.82 kcal g^{-1}, 10% fat, 20% protein, 70% carbohydrate; D12450H; Research Diets, Inc., New Brunswick, NJ, USA) and distilled water at all times. All animal studies were conducted under guidance of the animal care protocol approved by the Institutional Animal Care and Use Committee of Rutgers University (OLAW #A3262–01, protocol #13–001).

2.3. Pharmacokinetic Studies and Dosage Regimen

Two pharmacokinetic (PK) studies were carried out. In Study 1, male and female mice received LFD for 10 days and sex-matched animals were then randomly grouped (n = 3–5) for a single oral RK dose (200 mg kg^{-1}). In Study 2, male mice were fed either the LFD used in Study 1 or a polyphenol-free HFD (4.73 lccal g^{-1}, 45% fat, 20% protein, 35% carbohydrate; D12451; Research Diets, Inc., New Brunswick, NJ, USA) for 8 weeks before being grouped (n = 3–5) for a single oral RK dose (200 mg kg^{-1}). This dose was selected based upon the earlier findings that 4 weeks' oral administration of 200 mg kg^{-1} RK significantly reduced weight gain and white adipose mass in HFD-fed male mice compared with the controls.[9] For a 60-kg adult human, the dose was equivalent to roughly 973.2 mg of free RK per day to predict similar biological effects found in the animals. After an overnight fast (12 h), all animals were orally gavaged with RK (200 mg kg^{-1}) delivered through a vehicle solution (50% propylene glycol, 40% deionized water, and 10% DMSO). Oral gavage dosing was performed using single-use, sterile plastic feeding tubes (20 gauge × 30 mm; Instech Laboratories, Plymouth Meeting, PA, USA).

2.4. Sample Collection

Following dosing, blood and tissue specimens were collected at 15, 30 min, 1, 1.5, 2, 4, 6, and 12 h post-gavage. Vehicle dosed animals (n = 3) were sacrificed without RK dosing to obtain the baseline phenolic profile. To collect samples, mice were first anesthetized with isoflurane. Blood was then collected via cardiac puncture into heparinized tubes and centrifuged at 3000 × g for 10 min at 4 °C to isolate plasma. Following cardiac puncture, animals were exsanguinated, perfused with 0.9% saline and decapitated, and brain and epididymal adipose depot (male only) were excised. Tissues were immediately homogenized with 0.2% formic acid at 1:2 w/v. For urine collection, animals were individually housed in metabolic cages one day before the experiment. Urine was collected during the overnight fast for baseline determination, and excretion was collected from the same animals again 12 h after RK administration. Plasma and urine were acidified with 2% formic acid to a final concentration of 0.2% v/v immediately upon collection. All biological specimens were stored at −80 °C until analysis.

2.5. Extraction of RK and Metabolites in Biological Samples

2.5.1. Plasma, Brain, and Urine—On the day of extraction, all specimens were thawed on ice, and extractions were then performed at room temperature. Two internal

standards (ISs), 4-hydroxybenzoic-2,3,5,6-d_4 (IS1), and *trans*-cinnamic acid-d_7 (IS2) (≈2 μg mL^{-1} each), were first diluted in 0.4 m NaH_2PO_4 bufFer (pH 5.4) and then added to an aliquot of plasma (100 μL), urine (100 μL), and brain homogenate (500 μL), to a final concentration of ≈200 ng mL^{-1}. The mixture was mixed with 300 μL (for plasma and urine) or 500 μL (for brain) of NaH_2PO_4 buffer and then digested with 100 μL (plasma) or 200 μL (brain and urine) of the solution of *β*-glucuronidase (2000 U) in contamination with sulfatase diluted in NaH_2PO_4 buffer at 37 °C for 45 min after purging with nitrogen. Enzymatic reaction was stopped by adding ethyl acetate (500 μL) and mixed by vortexing vigorously for 1 min, followed by centrifuging at 8000 × *g* for 5 min. The upper organic phase was transferred to a disposable glass tube, followed by adding 20 μL of 2% ascorbic acid in methanol. After two more extractions with ethyl acetate (500 μL each), the pooled supernatant was dried under a gentle stream of nitrogen at room temperature. The residue was reconstituted in 200 μL of 60% methanol containing 0.1% formic acid and centrifuged at 16 500 × *g* for 15 min before analyzed by UPLC-QqQ/MS.

2.5.2. Adipose Tissue—Due to the excess amount of lipid content in the adipose tissue, a post clean-up step was employed to remove the undesired lipid content. In brief, homogenized adipose specimens were thawed on ice, and an aliquot (250 μL) of sample was spiked with ISs as aforementioned. The mixture was mixed with 350 μL of NaH_2PO_4 buffer and then digested with 100 μL of enzyme solution (2000 U). Enzymatic reaction was stopped by adding 500 μL of methanol containing 4% HC1, followed by vortexing and sonicating in ice water bath for 5 min. After centrifugation at 16 500 × *g* for 5 min at 4 °C, 750 μL of supernatant were collected in a glass tube containing 20 μL of 2% ascorbic acid. After one more extraction with acidified MeOH (500 μL), the pooled MeOH extract (1.5 mL) was transferred to a 5-mL centrifugal tube and washed with same volume of *n*-hexane by inverting the vial several times. The lower clear MeOH layer was collected after centrifugation at 8000 × *g* for 5 min and then dried under a gentle stream of nitrogen. The residue was reconstituted in 640 μL pure ACN acidified with 1% formic acid to precipitate salts and centrifuged at 16 500 × *g* for 5 min. The supernatant was then transferred to another tube containing 160 μL water with 1% formic acid. The mixture was passed through Captiva EMR-Lipid filters (96-well plate, Agilent Technology, Santa Clara, CA, USA) to remove the remaining lipids. The filter wells were washed twice with 250 pL of 75% ACN containing 1% formic acid. The eluents collected were dried under nitrogen, reconstituted in 100 μL of 60% MeOH containing 0.1% formic acid, and centrifuged at 16 500 × *g* for 15 min at 4 °C before being analyzed by UPLC-QqQ/MS.

2.6. Instrumentation and Analytical Methods

The analyses of RK and its structurally related metabolites were carried out on an Agilent 1290 Infinity II UPLC system interfaced with an Agilent 6470 triple quadrupole mass spectrometer with an electrospray ionization (ESI) source (Agilent Technology, Palo Alto, CA, USA).

Chromatographic separation was achieved using a Waters Acquity UPLC BEH C18 column (2.1 × 50 mm, 1.7 μm) (Milford, MA, USA) equipped with a Waters VanGuard Acquity C18 guard column (2.1 × 5 mm, 1.7 μm). The binary mobile phase system consisted of phase A

(0.1% AA in water) and phase B (0.1% AA in ACN). The flow rate was set at 0.45 mL min $^{-1}$. The gradient elution program for each run started at 5% (B%), followed by 10% at 0.5 min, 28% at 3.8 min, 40% at 3.9 min, 55% at 5.5 min, 80% at 5.6 min, and then held isocratically until 6 min. The column was equilibrated for 2.5 min before the next injection. Thermostats of the column and the autosampler were set at 30 and 4 °C, respectively. Injection volume was 3.5 μL for all standard solutions and sample: extracts.

Mass spectral data acquisition was achieved using dynamic multiple reaction monitoring with switching polarities. Two specific transitions for each analyte were monitored over a period of 1 min centered around retention time. The ESI parameters were set as follows: dry gas at 250 °C with a flow rate of 12.0 L min^{-1}, sheath gas at 250 °C with a flow rate of 12.0 L min^{-1}, nebulizer at 30 psi, nozzle voltage at +1.5 kV/–1.0 lcV and capillary voltage at +3.0 kV/–2.5 kV. Identification and confirmation of target compounds were determined by comparing their MRM precursor—product ion pair transition(s) and the retention time with those of authentic standards. Detailed compound information and MRM transitions are displayed in Table S1, Supporting Information. Quantitation was achieved with calibration curves established using the peak area ratio of analyte-to-IS of the quantifier ions.

2.7. Statistics

All phenolic extracts from plasma, urine, and tissue specimens were injected twice into the LC-MS/MS in a random manner, and a tracker consisting of all phenolic analytes and ISs prepared at a concentration of 1000 ng mL^{-1} was injected every 15 samples to monitor potential compound degradation during sequential runs. Pharmacokinetic parameters including area under the concentration-versus-time curve ($AUC_{0–12\ h}$), maximum concentration (C_{max}), time to reach maximum concentration (T_{max}), and elimination half-life ($T_{1/2}$) were calculated using the piecewise cubic interpolation method in MATLAB (ver. 2018a, The MathWorks Inc., USA). The data were subjected to Student's *t*-test, one-way ANOVA, and Pearson correlation analyses using the R software.[17]

3. Results

3.1. Animal Treatments, Food Intake, and Body Weight

Male and female mice were fed a polyphenol-free LFD in Study 1. Mean body weight (g ± SEM) was significantly higher for males (23.39 ± 0.45 g, $n = 27$) than females (16.49 ± 0.15 g, $n = 27$) ($p < 0.001$). Another cohort of male mice were exposed to a LFD or HFD for 8 weeks in Study 2. At the end of treatment period, the HFD-fed mice (37.32 ± 0.86 g, $n = 27$) gained significantly more weight than the LFD-fed mice (28.07 ± 0.47 g, $n = 27$) ($p < 0.001$) (Figure S1, Supporting Information).

3.2. Characterization of RK and Its Major Metabolites in Biological Fluids and Tissues from Mice Acutely Dosed with RK

As phenolic metabolites generated by cells or gut microbiota normally represent the predominant circulating phenols that can reach adequate levels to elicit a biological response at the site(s) of action, [18,19] we performed preliminary studies to identify the primary metabolites of RK in the plasma of normal-weight mice given an acute dose of RK. We were

able to tentatively identify 29 phenolic compounds as RK metabolites (Table S1, Supporting Information). Among the 30 analytes surveyed, 28 were detected in plasma (except 3-hydroxycinnamic acid), and 16 were found in the brain and 22 in epididymal adipose tissue, either as endogenous compounds and/or RK-derived metabolites. Results revealed that concentrations of 17 analytes significantly increased by certain time-points post-administration compared with baseline levels ($p < 0.05$), which include 9 RK-specific metabolites (RSMs), that is, 4 phenyl alcohols and 5 phenyl aldehydes, and 8 referenced microbial-derived phenolic acid metabolites (PAMs). There appears to be highly positive correlations among the concentrations of RK and its potential metabolites (Figure 5), thus providing evidence to propose the formation of RK-derived metabolites following oral ingestion. For all animals, the most bioavailable compounds are RK and raspberry alcohol (ROH), followed by 4-hydroxyphenylethanol (4-HPE), 4-hydroxyphenylacetic acid (4-HPAA), and vanillylacetone (VLAce) (Tables 1 and 2). Representative LC-MS chromatograms of select phenolic analytes detected in plasma of male mice, as shown in Figure 1, illustrate the observed increases and decreases in RK and ROH levels at specific time points following administration. In 12-h urine excretion, we detected all target analytes except 3-hydroxybenzoic acid (3-HBA) and 3-hydroxycinnamic acid. Apart from RK, the predominant metabolites detected in urine of all cohorts were RSMs, that is, ROH, 4-HPE, 2-(3,4-dihydroxyphenyl)ethanol (3,4-DHPE), 3,4-dihydroxybenzylideneacetone (DHPhLiAce), VLAce, vanillylideneacetone (VLiAce), methylated raspberry ketone (RK-Me), and a PAM (4-HPAA) (Table S7, Supporting Information).

3.3. Plasma Pharmacokinetics and Brain Distribution of RK and Its Metabolites in Male and Female Mice (Study 1)

Concentrations of RK and its major metabolites in plasma and brain of normal-weight mice following RK administration are presented in Tables S2 and S3, Supporting Information, respectively. The representative PK curves of RK, ROH, and RK-Me in plasma and brain are illustrated in Figure 2, with PK parameters detailed in Table 1. Following acute RK administration, both male and female mice quickly absorbed RK and metabolized it into diverse structurally related metabolites. In general, RK and most of its metabolites were present in bloodstream at considerably higher levels than the baseline within 30 min and returned to baseline in 6 h. Maximal plasma concentrations (C_{max}) of RK and ROH arrived at 15 and 25 min, respectively, for both sexes, while C_{max} values were considerably higher in females. For the rest of RSMs, peak values generally arrived within 40 min. Similarly, females exhibited faster metabolism and circulation of RK metabolites than their counterparts, but all were accompanied by shorter elimination half-time (<50 min), except 4-HPE and 3,4-DHPE. This explains, at least in part, the slightly lower bioavailability of RK in females than males, as estimated by the cumulative $AUC_{0–12\ h}$ including RK and its seven major RSMs (566 vs 675 nmol mL^{-1} min^{-1}) (Table 1). For other phenolic metabolites, we observed evident elevation in plasma levels of 4-H PPA 3-HPPA, 4-HPAA, 4-HCA, VA, and HVA compared with the baseline (Table S2, Supporting Information). Regarding the brain, deposition levels of RK, ROH, 4-HPE, VLAce, 4-HBA, 4-HPAA, and HVA were in the nmol/g tissue range, and the rest of the metabolites detected were at sub-nmol/g level (Table S3, Supporting Information), while some plasma-targeting metabolites including RK-Me, benzylideneacetone, ferulic acid (FA), and 3-(3-hydroxyphenyl)propionic acid (3-HPPA)

were not found in the brain of either sexes. The T_{max} values of RKand RSMs in both cohorts mostly fall in the range of 15–30 min post-dosing (Table 1). Regarding PAMs, they peaked at later time points and their concentrations varied much less relative to RSMs. In both plasma and brain, however, total bioavailability of RK was not statistically different between females and males.

3.4. Plasma Pharmacokinetics and Tissue Distribution of RK and Its Metabolites in Normal-Weight and Obese Mice (Study 2)

As shown in PK curves and parameters of RK, ROH, and RK-Me (Figure 3 and Table 2), for normal-weight animals, plasma levels of RK and major RSMs peaked between 15 min and 1 h, while there appeared to be a delay in metabolism and distribution of RSMs in the obese cohort, especially for ROH, VLAce, and VLiAce. T_{max} for PAMs generally ranged between 30 min and 1 h for both cohorts, with significantly higher generation of 4-HPAA and 4-HCA in obese mice. Striking differences between normal-weight and obese animals lie in the PK behaviors of RK and major RSMs (Table 2). Obese animals showed higher capacity to absorb and retain RK and some metabolites (ROH, 4-HPE, 3,4-DHPE, DHPhLiAce, and VLAce), resulting in significantly higher peak concentrations, longer elimination half-lives, and considerable amount of residual phenolics, for example, RK level at 12 h was ≈20-fold that of the normal mice and ≈10 folds for RSMs in plasma (Table S4, Supporting Information). Considering brain levels (Table S5, Supporting Information), similar trends were observed between the two cohorts. In particular, accumulation of RK, ROH, 4-HPE, and VLAce was significantly higher in the brain of obese mice ($p < 0.01$) but were at retarded peaking and elimination rates. These may collectively contribute to the significantly higher total bioavailability ($AUC_{0–12\ h}$) in obese compared with the non-obese cohorts (1197 vs 679 nmol mL^{-1} min^{-1}, $p < 0.01$).

We also extracted, using a different liquid—liquid extraction method with additional lipid removal steps, and chemically profiled all phenolic analytes in a representative WAT in male animals, i.e, the epididymal adipose tissue, and results are presented in Figure 4. Considerable accumulation of RK in WAT were observed within 15 min as well as its major metabolites, including ROH, RK-Me, 4-HPE, DHPhLiAce, VLAce, and VLiAce (Table S6, Supporting Information). As hypothesized, WAT from obese mice took up more RK and almost all major RSMs throughout the course of observation compared with the normal-weight ones. In particular, there were 30–90% increases in RK and ROH levels between 15 and 30 min in obese animals. After 30 min, phenolic efflux rates appeared to be significantly lower in obese groups than their normal-weight counterparts ($p < 0.05$, Figure 4), resulting in a >100% higher residual RKand RSM contents in obese mice between 30 min and 2 h. In addition, very low proportions of PAMs were present in WAT compared to that in other biosamples including the brain (Figures 3 and 4). Yet, total phenolic accumulation in the brain was much lower than that in WAT for both obese and normal-weight cohorts.

Metabolites with significant and/or detectable deposition in plasma, brain, and WAT generally displayed synchronized changes in concentration as shown in Figure S2, Supporting Information, suggesting active exchange of metabolites among blood and select tissues during the course of observation. Brain and WAT levels of RK and its predominant

metabolite, ROH, for example, exhibited strong dependence on plasma level (Pearson correlation 0.80–0.92, in an exponential manner), and significant elevation in brain and WAT concentrations was most prominent when respective plasma concentration increased to 10 nmol mL^{-1} or above.

4. Discussion

In recent years, RK has been shown to be effective in preventing weight gain in rodent models of diet-induced obesity.[9] In addition, RK has been marketed as a dietary supplement for weight loss but the recommended dosages are exceedingly high compared with the estimated dietary exposure.[16] Scarce information is available on RK's oral bioavailability and metabolism in vivo, which is essential for elucidating the sites and mechanisms of action of RK as well as its oral toxicity. Our studies examined whether there was a sex-dependent or diet-induced obesity effect on the bioavailability and metabolism of RK in mice. In this work, RK pharmacokinetic studies were conducted over a period of 12 h after a single oral dose, followed by analyzing RK and 29 metabolites in plasma, brain, WAT, and urine samples using a targeted metabolomic approach (Table S1, Supporting Information).

Based on our earlier findings, daily oral administration of 200 mg kg^{-1} for 4 weeks significantly reduced weight gain and white adipose mass in HFD-fed male mice compared with the vehicle.[9] In addition, preliminary dosing tests conducted in normal-weight male mice indicated >99% clearance of RK from the bloodstream in 24 h. As such, we selected the 200 mg kg^{-1} dose and collected samples during a period of 12 h for bioanalysis.

The ADME of phenolic compounds begins with absorption primarily in the upper intestine, followed by extensive first-pass metabolism by enterocytes and hepatocytes prior to systemic circulation and tissue distribution. In this study, we observed fast absorption and tissue accumulation of RK (<30 min). According to plasma PK parameters, maximal circulating concentration of RK attained 236 nM for normal-weight and 318 nM for obese mice. In addition, RK was efficiently converted into structurally related metabolites in all animal cohorts. Among the 29 metabolites surveyed, 17 exhibited synchronized changes in plasma concentration with that of RK, demonstrating strong associations with RK absorption and metabolism (Figure 5). These findings are encouraging as poor bioavailability has long been a conundrum in utilizing bioactive phytochemicals as prophylactic agents.[20,21] In the study by Sporstøl and Scheline, analyses of 0–24 h urinary excretion partly revealed the metabolic fate of RK in rats, guinea pigs, and rabbits following a single intragastric dose of RK (164 mg kg^{-1}).[11] In line with their findings, RK catabolism was orchestrated by intracellular ketone reduction and methylation, microbial (de)hydroxylation, demethylation, decarboxylation, and hydrogenation. Our studies further confirmed the bioconversion of RK into metabolites including RK-Me, ROH, 4-HPE, VLAce, and a few PAMs although no diols were detected in any samples using MRM scan. In addition, we report a far greater array of metabolites, that is, 20 more new metabolites (Table S1, Supporting Information). Based on current knowledge, we propose the metabolic pathways of RK in mice (Figure 6). However, as all samples were processed with deconjugating enzymes, no glucuronidated/sulfated metabolites could be detected.

In the context of metabolic disorders, sex-dependent differences should be carefully considered by running parallel experiments with both males and females. Metabolism and bioavailability of xenobiotics including phenolic compounds have been found to differ greatly between males and females.[22,23] For instance, males (rats, humans) tend to metabolize xenobiotics faster and more extensively than females. Tissue distribution of phenolics can also be distinct across sexes.[22,23] Moreover, differences in the gut microbiome across sexes have also been appreciated which can markedly alter the bioefficacy of compounds of interest.[24] In Study 1, however, RK and its major metabolites available in both plasma and brain were comparable between males and females (Table 1). When analyzing 12-h urinary outputs, however, we found that the recovery of RK, including seven major RSMs, in females (10.94%) was twice as much as in males (5.34%) (Table S7, Supporting Information). Our recovery percentage was far below that reported for the 24-h urine from rats,[11] and this can be partially explained by the differences in the ways of recovery calculation (including RK and all the proposed metabolites vs RK and select metabolites for recovery estimation), length of urinary excretion (24 h vs 12 h), analytical methods (GC-MS vs LC-QqQ/MS), and animal species (rat vs mouse). No considerable difference in urine recovery was observed between normal-weight (6.26%) and obese (8.30%) animals in Study 2.

Disease status such as obesity can largely affect the bioavailability of nutrients and phytochemicals,[15] which have been linked to the alterations in gut functions,[25] biological barriers,[12,13] xenobiotic metabolizing systems,[26] efflux transporter activities,[27] and gut microbiota.[25] In Study 2, animals fed a HFD for 8 weeks exhibited significantly higher body weight ($p < 0.001$) than those fed a LFD (Figure S1, Supporting Information), and in the meanwhile, exhibited significantly augmented RK bioavailability ($p < 0.001$) (Table 2). Twelve-hour plasma accumulation of RK in obese animals was 152.2–197.6% that of normal-weight ones, and similar trends applied to total phenol deposition levels. In line, for tissue samples, RK and its major metabolites exhibited significantly higher bioavailability and extended half-life in obese animals compared with their normal-weight counterparts (Figures 3 and 4). The estimated plasma bioavailability and C_{max} of obese mice were 1.76- and 1.35-folds that of normal-weight mice, respectively (Table 2). As a referenced consequence of chronic obesogenic diet intake, the subsequent disruption of tight junctions in the intestinal walls (the so-called “leaky gut”)[28] and in the blood-brain barrier,[29] could allow more xenobiotics to enter systemic circulation and deposit in tissues. The delayed T_{max} and $T_{1/2}$ could also be partly due to extended intestinal transit time which slows down the absorption and metabolism of phenolics.[15] In line with these findings, Margalef et al. observed elevated bioavailability of grape flavanols and their metabolites in plasma and a 2-h delay of T_{max} in obese rats with metabolic syndromes compared to control rats.[30] Yet, discrepancies have also been observed in PK studies involving animals or humans with metabolic syndromes. For example, Chen et al. reported that diabetic Zuclcer rats exhibited decreased overall bioavailability and first-pass metabolism of polyphenols in the plasma and brain following ingestion of a grape polyphenol mixture, which was ascribed to higher urinary clearance of polyphenols due to osmotic diuresis, and possible changes in key polyphenol transporters and metabolizing enzymes.[13] A comparison of two clinical studies on the PK parameters of *trans*-resveratrol between non-obese and obese cohorts reveals

strikingly higher C_{max}/dose and AUC/dose in non-obese participants.[31,32] Furthermore, inspired by promising in vitro results that the underlying anti-obesity mechanisms of RK could be its capacity to enhance lipolysis, WAT browning, and fatty acid oxidation,[7,33,34] we also sought to find out whether HFD-induced obesity also alters deposition of these phenolics in WAT. A striking difference in the accumulation of phenolics in WAT as compared with in bloodstream and brain is that WAT appears to retain RK and RSMs at a higher proportion of total phenolics and for longer periods (Table 2 and Table S6, Supporting Information), possibly due to the affinity of these lipophilic molecules to adipocytes and lower efflux efficiency in WAT. In addition to RK, two predominant RSMs, that is, 4-HPE (known as tyrosol)[35] and VLAce (known as zingerone),[36] have also been reported to be lipolytic or anti-adipogenic in vitro. In view of the remarkable accumulation of RK together with its RSMs in epididymal adipose tissue, RK-related phenolics may potentially target WAT to favorably alter adipose distribution and functionality of different fat depots.

5. Concluding Remarks

In the present work, two PK studies were carried out to examine the bioavailability and metabolism of RK in four cohorts of mice, that is, male versus female and normal weight versus obese. Using a targeted metabolomic approach, we surveyed 29 potential metabolites in addition to the precursor compound in plasma, brain, WAT, and urine to comprehensively understand the ADME of this natural phenolic compound with obesity-preventative potential. There were no significant differences in the overall RK bioavailability across sexes. However, the overall bioavailability was remarkable elevated in HFD-induced obese than normal-weight animals while the absorption and metabolism of RK were generally delayed. In view of the remarkably fast absorption, high oral bioavailability of RK, and accumulation in lipid-rich tissues, that is, brain and WAT, the application of RK as a potential obesity-preventative agent may be effective at lower doses than those advertised in marketed RK dietary supplements. Furthermore, we have synthesized the ^{13}C-labeled RK molecule and anticipate confirming the actual metabolic pathways of RK in normal-weight mice next.

A major limitation of this study is the lack of information on phase II metabolites of RK as the xenobiotic metabolism and efflux systems have also been reported to undergo intrinsic alterations during the development of obesity. The lack of information regarding the concentration of RK and its major metabolites in the liver is another caveat in our study. Although structural information of RK metabolites are hardly available in the literature, it is worthwhile to assess the potential of major RK phase II or microbial metabolites in preventing or attenuating obesity-related risk factors. Another limitation is that vaginal cytology was not performed at sacrifice to determine the stage of estrous cycle in female animals which may greatly influence their metabolism.[37] Further studies in relation to the generation of WAT and/or brain-targeting bioactive RK metabolites, and phylogenomic analysis of microbial communities in response to RK administration are warranted.

Supplementary Material

Refer to Web version on PubMed Central for supplementary material.

Acknowledgements

This work was supported by the NIH-NCCIH R01AT008933, the associated Administrative Supplement grant 3 R01 AT008933-03S1 and USDA-NIFA NJ06280. The authors would like to thank Xinyi Li and Aditi Badrinath for their technical assistance in animal experiments. The help from Peixuan Yuan with the calculation of pharmacokinetic parameters in MATLAB is also acknowledged. Preliminary data of this manuscript were presented at the American Society of Nutrition annual meeting 2019 in Baltimore MD, June 8–11, 2019.

References

[1]. Wu T, Yang L, Guo X, Zhang M, Liu R, Sui W, Food Funct. 2018, 9, 2112. [PubMed: 29632909]

[2]. Luo T, Miranda-Garcia O, Adamson A, Sasaki G, Shay NF, J. Berry Res. 2016, 6, 213.

[3]. Rao AV, Snyder DM, J. Agric. Food Chem. 2010, 58, 3871. [PubMed: 20178390]

[4]. Istas G, Feliciano RP, Weber T, Garcia-Villalba R, Tomas-Barberan F, Heiss C, Rodriguez-Mateos A, Arch. Biochem. Biophys. 2018, 651, 43. [PubMed: 29802820]

[5]. Törrönen R, Kolehmainen M, Sarkkinen E, Poutanen K, Mykkänen H, Niskanen L, J. Nutr. 2013, 143, 430. [PubMed: 23365108]

[6]. Opdyke DLJ, Food Cosmet. Toxicol. 1978, 16, 781.

[7]. Leu SY, Tsai YC, Chen WC, Hsu CH, Lee YM, Cheng PY, J. Nutr. Biochem. 2018, 56, 116. [PubMed: 29525531]

[8]. Leu S-Y, Chen Y-C, Tsai Y-C, Hung Y-W, Hsu C-H, Lee Y-M, Cheng P-Y, Agric J. Food Chem. 2017, 65, 10907.

[9]. Kshatriya D, Li X, Giunta GM, Yuan B, Zhao D, Simon JE, Wu Q, Bello NT, Nutr. Res. 2019, 68, 19. [PubMed: 31252376]

[10]. Arent SM, Walker AJ, Pellegrino JK, Sanders DJ, McFadden BA, Ziegenfuss TN, Lopez HL, J. Am. Coll. Nutr. 2018, 37, 111. [PubMed: 29111889]

[11]. Sporstøl S, Scheline RR, Xenobiotica 1982, 12, 249. [PubMed: 7113261]

[12]. Margalef M, Pons Z, Iglesias-Carres L, Quiñones M, Bravo FI, Arola-Arnal A, Muguerza B, Mol. Nutr. Food Res. 2017, 61, 1600342.

[13]. Chen TY, Ferruzzi Mario G, Wu QL, Simon James E, Talcott Stephen T, Wang J, Ho L, Todd G, Cooper B, Pasinetti Giulio M, Janie Elsa M, Mol. Nutr. Food Res. 2017, 61, 1700111.

[14]. Blouin RA, Warren GW, J. Pharm. Sci. 1999, 88, 1. [PubMed: 9874695]

[15]. Redan BW, Buhman KK, Novotny JA, Ferruzzi MG, Adv. Nutr. 2016, 7, 1090. [PubMed: 28140326]

[16]. BredsdorfF L, Wedebye EB, Nikolov NG, Hallas-Møller T, Pilegaard K, Regul. Toxicol. Pharmacol. 2015, 73, 196. [PubMed: 26160596]

[17]. R Core Team, R: A language and environment for statistical computing, R Foundation for Statistical Computing, Vienna, Austria 2013.

[18]. Rein MJ, Renouf M, Cruz-Hernandez C, Actis-Goretta L, Thakkar SK, da Silva Pinto M, Br. J. Clin. Pharmacol. 2013, 75, 588. [PubMed: 22897361]

[19]. Zhao D, Simon J, Wu Q, Crit. Rev. Food Sci. Nutr. 2020, 60, 597.

[20]. Del Rio D, Borges G, Crazier A, Br. J. Nutr. 2010, 104, S67. [PubMed: 20955651]

[21]. Yang CS, Sang S, Lambert JD, Lee M-J, Mol. Nutr. Food Res. 2008, 52, S139. [PubMed: 18551457]

[22]. Bock M, Thorstensen EB, Derraik JGB, Henderson HV, Hofman PL, Cutfield WS, Mol. Nutr. Food Res. 2013, 57, 2079. [PubMed: 23766098]

[23]. Margalef M, Pons Z, Iglesias-Carres L, Arola L, Muguerza B, Arola-Arnal A, Mol. Nutr. Food Res. 2016, 60, 760. [PubMed: 26799813]

[24]. Tomás-Barberán FA, García-Villalba R, González-Sarrías A, Selma MV, Espín JC, J. Agric. Food Chem. 2014, 62, 6535. [PubMed: 24976365]

[25]. Hartstra AV, Bouter KEC, Bäckhed F, Nieuwdorp M, Diabetes Care 2015, 38, 159. [PubMed: 25538312]

[26]. Liu H, Wu B, Pan G, He L, Li Z, Fan M, Jian L, Chen M, Wang K, Huang C, Drug Metab. Dispos. 2012, 40, 2109. [PubMed: 22859782]

[27]. Yu S, Yu Y, Liu L, Wang X, Lu S, Liang Y, Liu X, Xie L, Wang G, Planta Med. 2010, 76, 876. [PubMed: 20108175]

[28]. Harris K, Kassis A, Major G, Chou CJ, J. Obes. 2012, 2012, 14.

[29]. Davidson TL, Monnot A, Neal AU, Martin AA, Horton JJ, Zheng W, Physiol. Behav. 2012, 107, 26. [PubMed: 22634281]

[30]. Margalef M, Pons Z, Iglesias-Carres L, Bravo FI, Muguerza B, Arola-Arnal A, Food Chem. 2017, 231, 287. [PubMed: 28450008]

[31]. Chachay VS, Macdonald GA, Martin JH, Whitehead JP, O'Moore—Sullivan TM, Lee P, Franklin M, Klein K, Taylor PJ, Ferguson M, Coombes JS, Thomas GP, Cowin GJ, Kirkpatrick CMJ, Prins JB, Hickman IJ, Clin. Gastroenterol. Hepatol. 2014, 12, 2092. [PubMed: 24582567]

[32]. Boocock DJ, Faust GES, Patel KR, Schinas AM, Brown VA, Ducharme MP, Booth TD, Crowell JA, Perloff M, Gescher AJ, Steward WP, Brenner DE, Cancer Epidemiol. Biomarkers Prev. 2007, 16, 1246. [PubMed: 17548692]

[33]. Park KS, Pharm. Biol. 2015, 53, 870. [PubMed: 25429790]

[34]. Leu SY, Chen YC, Tsai YC, Hung YW, Hsu CH, Lee YM, Cheng PY, Agric J. Food Chem. 2017, 65, 10907.

[35]. Lee O-H, Kwon Y-I, Apostolidis E, Shetty K, Kim Y-C, Phytother. Res. 2011, 25, 106. [PubMed: 20623718]

[36]. Ahmad B, Rehman MU, Amin I, Arif A, Rasool S, Bhat SA, Afzal I, Hussain I, Bilal S, Mir M.u R., Sci. World J. 2015, 2015, 6.

[37]. Wade GN, Schneider JE, Neurosci. Biobehav. Rev. 1992, 16, 235. [PubMed: 1630733]

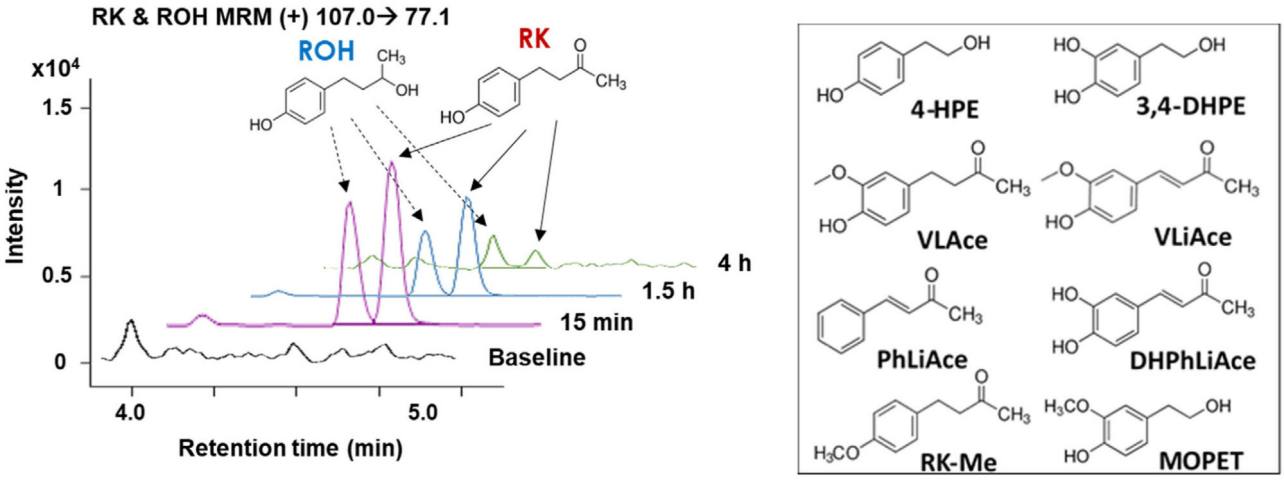

Figure 1.

Representative MS chromatograms of raspberry ketone (RK) and raspberry alcohol (ROH) detected in plasma of normal-weight male mice. Molecular structures of RK and ROH are shown above the chromatograms and other major RK-specific metabolites in the right panel. Samples were collected at baseline (black line), 15 min (pink line), 1.5 h (blue line), and 4 h (green line) post-gavage. MOPET, homovanillyl alcohol. Refer to Table 1 for abbreviation of other RSMs.

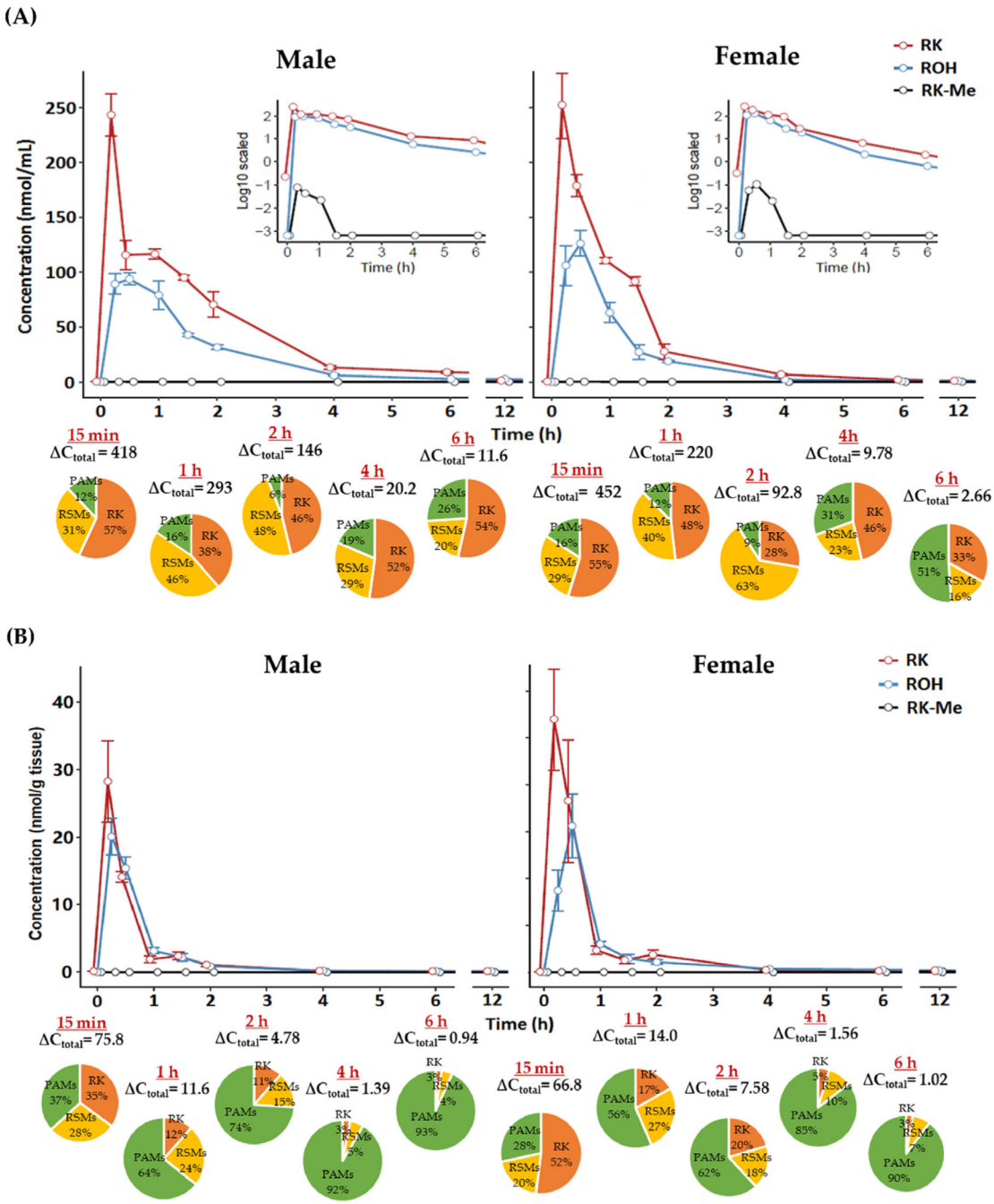

Figure 2.

Pharmacokinetic curves of raspberry ketone (RK), raspberry alcohol (ROH) and methylated raspberry ketone (RK-Me) in A) plasma (inset: concentrations in log scale) and B) brain in male and female mice dosed with RK; pie charts indicate profile of different phenolic categories (expressed as percentage of total phenols). ΔC_{total}, net change in total phenol concentration versus baseline. Data are expressed as mean ± SEM (n = 3–5). RSMs, RK-specific metabolites; PAMs, phenolic acid metabolites.

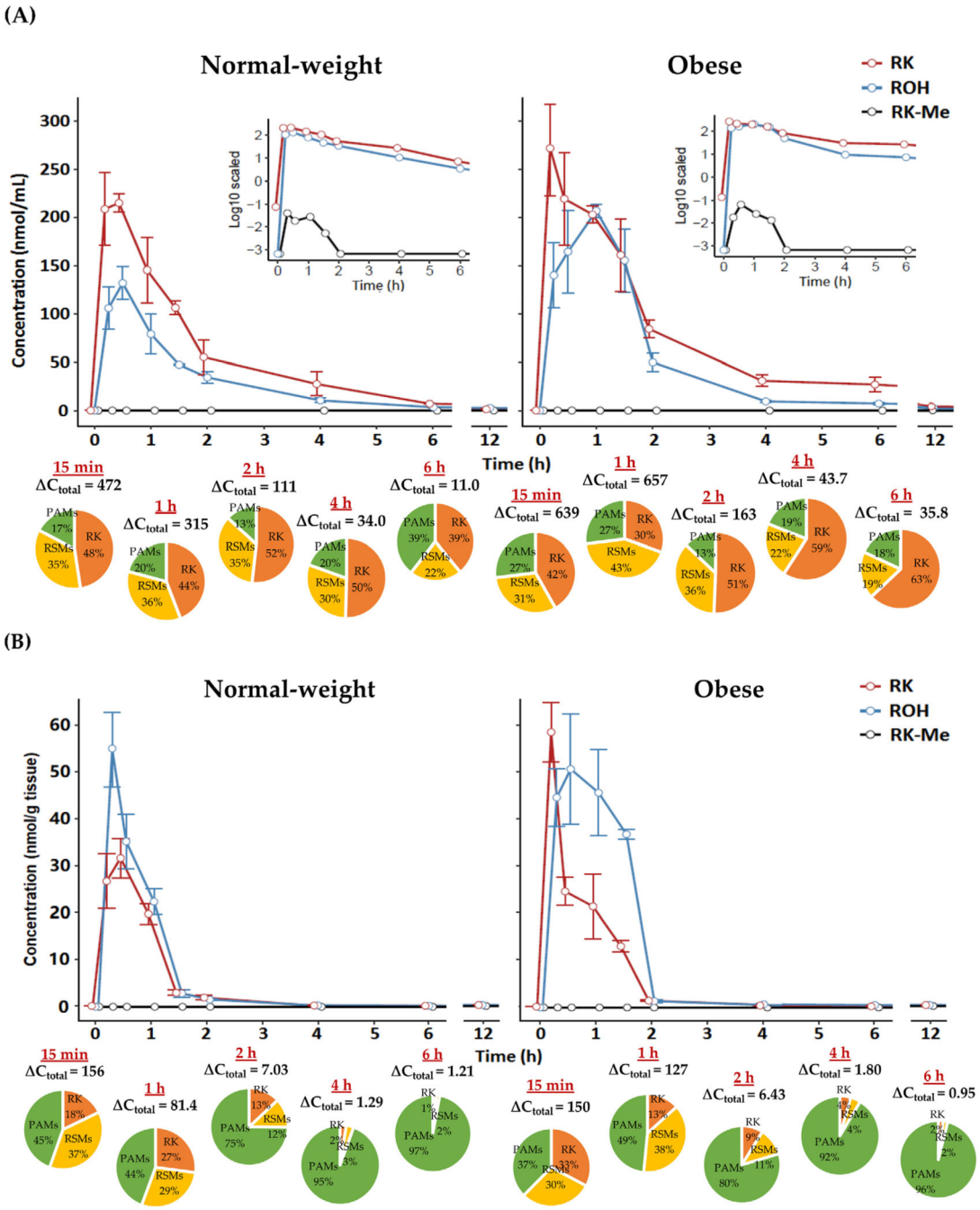

Figure 3.

Pharmacokinetic curves of RK, ROH, and RK-Me in A) plasma (inset: concentrations in log scale) and B) brain in normal-weight and obese male mice dosed with RK; pie charts indicate profile of different phenolic categories. ΔC_{total}, net change in total phenol concentration versus baseline. Data are expressed as mean ± SEM (n = 3–5).

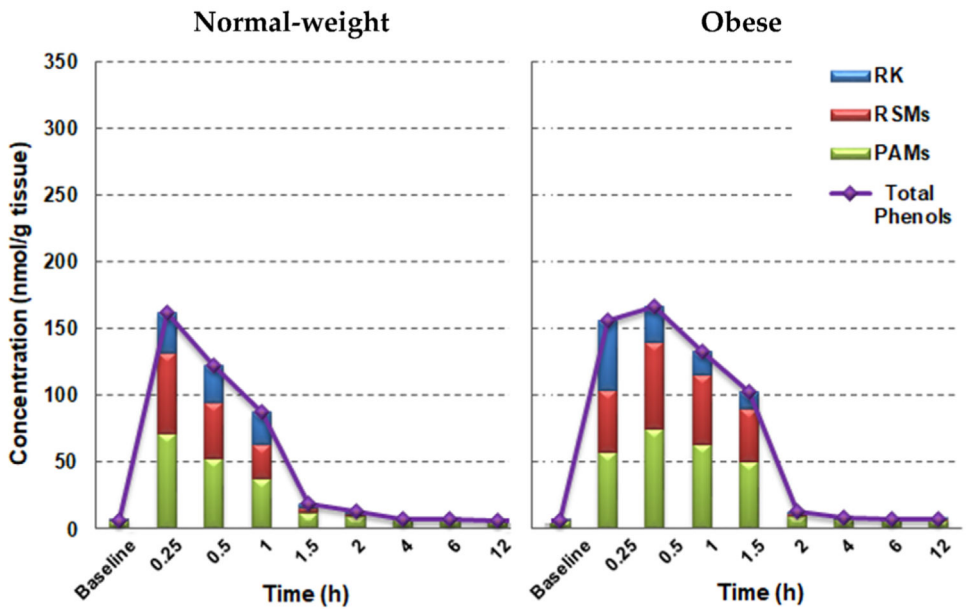

Figure 4.

Distribution of RK, RSMs (RK-specific metabolites), and PAMs (phenolic acid metabolites) in epididymal adipose tissue from normal-weight and obese male mice acutely dosed with RK. Data are expressed as mean concentrations (n = 3–5).

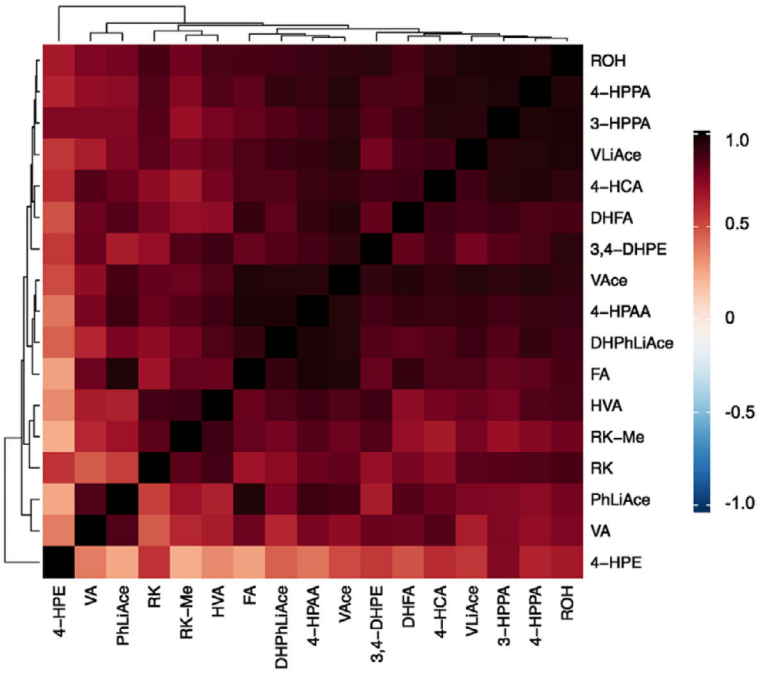

Figure 5.

Heatmap visualization of Pearson correlation of plasma level of raspberry ketone (RK) and its structurally related metabolites, showing concurrent changes in concentration after an acute dose of RK in normal-weight male mice. Compound abbreviations in addition to those in Table 1. 4-HCA, *trans-p*-Coumaric acid; 4-HPAA, 4-hydroxyphenyl acetic acid; 4-HPPA, 3-(4-hydroxyphenyl)propionic acid; 3-HPPA, 3-(3-hydroxyphenyl)propionic acid; VA, vanillic acid; HVA, homovanillic acid; FA, ferulic acid; DHFA, dihydroferulic acid.

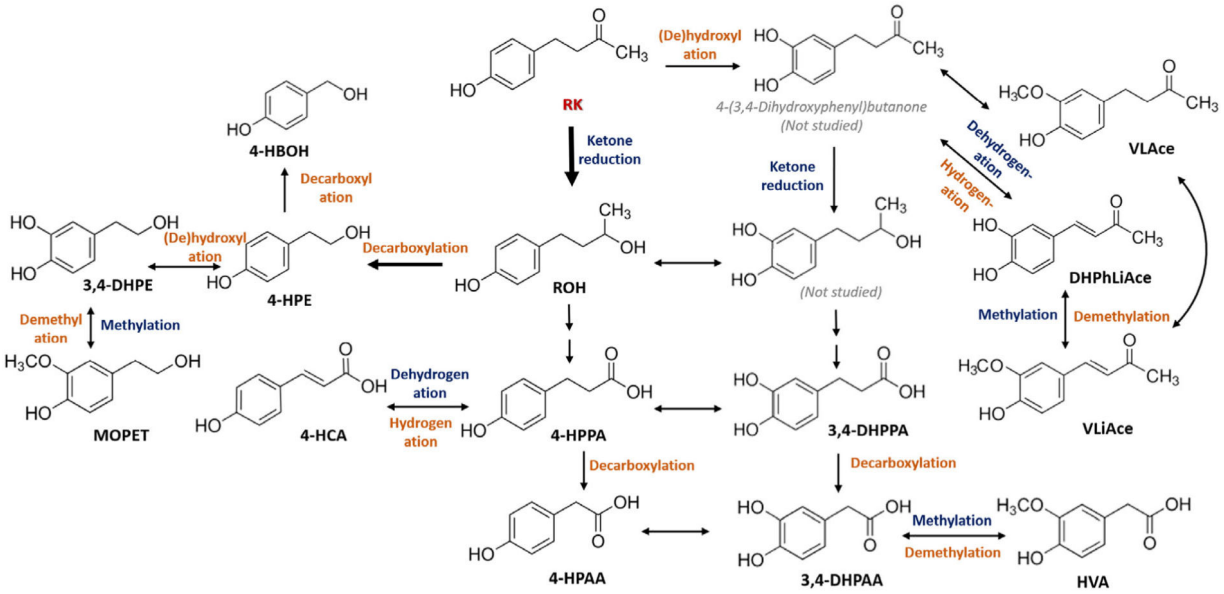

Figure 6.

Proposed metabolic pathways of raspberry ketone (RK) in mice. Phase I/II xenobiotic metabolism steps are indicated in dark blue and microbial metabolism steps are in orange.

Table 1.

a and brain pharmacokinetic parameters of raspberry ketone (RK) and major metabolites in male and female mice following acute RK istration.

ound	C_{max} [nmol mL^{-1}][a)]				T_{max} [min]				$T_{1/2}$ [min]				AUC [nmol mL^{-1} min^{-1}][a)]			
	Pl-M	Pl-F	Br-M	Br-F	Pl-M	Pl-F	Br-M	Br-F	Pl-M	Pl-F	Br-M	Br-F	Pl-M	Pl-F	Br-M	Br-F
	243±19.6	281±17.1	28.9±2.42	37.4±8.73	15.0±0.0	15.0±0.0	15.0±0.0	15.0±0.0	78.4±3.55	48.1 ** ±0.98	25.7±2.0	28.3±1.65	358±34.0	299±20.2	19.4±2.42	20.2±6.72
Me	0.079±0.012	0.086±0.022	–	–	20.0±5.0	25.0±5.0	–	–	26.7±2.81	31.4±1.84	–	–	0.050±0.005	0.069±0.010	–	–
	103±3.26	130±12.7	21.0±2.68	21.6±4.72	25.0±4.99	25.0±4.99	20.0±5.0	30.0 ** ±0.0	63.2±2.61	44.8 ** ±1.16	32.0±0.77	40.2 * ±1.66	177±11.8	158±17.1	18.8±1.65	19.4±3.34
E	41.8±3.73	43.6±2.90	1.03±0.14	1.28±0.08	50.0±9.98	40.0±10.0	15.0±0.0	20.0±5.0	104±2.10	117 * ±0.64	64.7±7.78	81.4 * ±4.44	108±10.9	98.7±7.38	1.58±0.16	2.24 *±0.14
HPE	0.055±0.013	0.024±0.002	0.021±0.003	0.020±0.006	20.0±5.0	15.0±0.0	15.0±0.0	15.0±0.0	41.8±1.25	63.6±6.84	21.0±0.16	20.3±1.41	0.057±0.006	0.031 * ±0.003	0.016±0.001	0.014±0.002
LiAce	0.48±0.06	0.25 *±0.04	0.067±0.011	0.112±0.042	40.0±10.0	15.0±0.0	20.0±5.0	25.0±4.99	41.4±2.91	30.0±4.24	33.4±0.73	35.8±2.29	0.465±0.046	0.156 * ±0.013	0.096±0.009	0.101±0.027
e	25.0±2.90	9.94±2.40	1.51±0.15	1.49±0.30	25.0±5.0	15.0±1.25	15.0±0.0	30.0 ** ±0.0	46.4±2.10	36.4 * ±2.80	84.1±3.55	89.2±10.0	31.0±3.65	9.98 **±1.74	1.98±0.16	1.76±0.27
ce	0.183±0.008	0.173±0.036	0.076±0.006	0.094±0.021	40.0±10.0	25.0±4.99	59.9±11.3	40.0±10.0	51.7±1.45	46.8±4.63	85.6±2.84	121 ** ±4.11	0.230±0.008	0.200±0.039	0.262±0.014	0.226±0.044
AUC													675±20.0	566±20.7	42.1±3.51	43.9±8.81

expressed as mean±SEM. A metabolite of RK is considered “major” if its concentration increased significantly at a certain time point compared with the baseline (vehicle-treated group), $p < 0.05$. group values are significantly different from male group at $p < 0.01$ (**), or $p < 0.05$ (*). C_{max}, maximum plasma concentration; T_{max}, time to reach C_{max}; $T_{1/2}$, elimination half-life; AUC, area e curve (0–12 h). Pl-M, plasma-male; Pl-F, plasma-iemale; Br-M, brain-male; Br-F, brain-female. ROH, raspberry alcohol; RK-Me, 4-(4-methoxy-phenyl)-2-butanone; 4-HPE, 2-(4-phenyl)ethanol; 3,4-DHPE, 2-(3,4-dihydroxyphenyl)ethanol; PhLiAce, benzylideneacetone; DHPhLiAce, 3,4-dihydroxybenzylideneacetone; VLAce, vanillylacetone; VLiAce, vanillylideneacetone.

f brain results is in nmol g^{-1}.

Table 2.

na and brain pharmacokinetic parameters of raspberry ketone (RK) and major metabolites in normal-weight and obese mice following acute RK nistration.

pound	C_{max} [nmol mL^{-1}]$^{a)}$				T_{max} [min]				$T_{1/2}$ [min]				AUC [nmol mL^{-1} min^{-1}]$^{a)}$			
	Pl-N	Pl-O	Br-N	Br-O	Pl-N	Pl-O	Br-N	Br-O	Pl-N	Pl-O	Br-N	Br-O	Pl-N	Pl-O	Br-N	Br-O
	236±20.0	318 *±23.5	32.7± 4.34	46.7±6.2	15.0±0.0	20.0± 5.0	20.0±5.0	20.0±5.0	73.3±1.2	94.7±7.8	39.5±1.9	41.5±4.0	387±25.6	675 **±37.2	33.7±2.3	42.8 *±2.0
Me	0.055±0.018	0.064±0.015	–	–	20.0±5.0	25.0±5.0	–	–	31.0±5.6	41.7±1.2	–	–	0.039±0.008	0.047±0.007	–	–
	149±15.0	212 *±6.7	55.1±8.12	60.3±6.6	25.0±5.0	50.0±10.0	20.0±5.0	40.0±10.0	66.1±1.7	70.0±1.5	33.7±2.2	52.4 ** ±1.88	208±22.0	391 **±15.8	34.8±3.8	76.8 *±6.6
PE	15.3±3.5	22.3±7.6	6.14±0.49	7.92±1.60	20.0±5.0	20.0±5.0	25.0±5.0	20.0±5.0	73.0±4.7	56.3±8.8	31.5±4.38	38.8±2.56	20.7±2.92	28.7±3.65	4.21±0.20	6.35±0.68
DHPE	0.074±0.017	0.147±0.031	0.031±0.003	0.025±0.002	20.0±5.0	25.0±5.0	20.0±5.0	20.0±5.0	48.9±6.9	51.7±4.36	35.5±3.94	33.2±2.3 5	0.080±0.006	0.162 ** ±0.011	0.024±0.002	0.021±0.002
hLiAce	0.99±0.12	1.29±0.10	0.23±0.012	0.16 *±0.010	30.0±0.0	40.0±10.0	30.0±0.0	20.0±5.0	41.6±3.0	48.0±2.1	36.2±1.6	37.2±0.22	1.04±0.16	1.38±0.04	0.19±0.022	0.15±0.012
ce	54.7±1.54	66.4 **±1.10	2.07±0.24	3.00 *±0.21	25.0±5.0	50.0±10.0	40.0±10.0	50.0±10.0	40.9±4.8	68.8±17.3	44.4±2.18	55.4 * ±0.76	61.2±4.7	99.1 **±5.6	2.20±0.21	3.22 *±0.16
Ace	0.36±0.027	0.35±0.062	0.14±0.038	0.08±0.005	30.0±0.0	50.0±10.0	50.0±10.0	80.0±10.0	47.7±2.85	63.3 * ±2.86	63.1±1.74	90.0 * ±4.46	0.41±0.02	0.52 **±0.04	0.17±0.027	0.16±0.007
AUC													679±17.2	1197 ** ±21.1	75.3±3.53	130±6.92

re expressed as mean±SEM. Obese group values are significantly different from normal-weight group at $p < 0.01$ (**), or $p < 0.05$ (*). C_{max}, maximum plasma concentration; T_{max}, time to reach $T_{1/2}$ elimination half-life; AUC, area-under-the-curve (0–12 h). Pl-N, plasma-normal-weight; Pl-O, plasma-obese; Br-N, brain-normal-weight; Br-O, brain-obese. ROH, raspberry alcohol; RK-Me, ethoxy-phenyl)-2-butanone; 4-HPE, 2-(4-hydroxyphenyl)ethanol; 3,4-DHPE, 2-(3,4-dihydroxyphenyl)ethanol; PhLiAce, benzylideneacetone; DHPhLiAce, 3,4-dihydroxybenzylideneacetone; e, vanillylacetone; VLiAce, vanillylideneacetone.

ofbrain results is in nmol g^{-1}.